Efficient Red Perovskite Light-Emitting Diodes Based on Solution-Processed Multiple Quantum Wells

Shuting Zhang, Chang Yi, Nana Wang, Yan Sun, Wei Zou, Yingqiang Wei, Yu Cao, Yanfeng Miao, Renzhi Li, Yao Yin, Ni Zhao, Jianpu Wang, and Wei Huang**

This paper reports a facile and scalable process to achieve high performance red perovskite light-emitting diodes (LEDs) by introducing inorganic Cs into multiple quantum well (MQW) perovskites. The MQW structure facilitates the formation of cubic $CsPbI_3$ perovskites at low temperature, enabling the Cs-based QWs to provide pure and stable red electroluminescence. The versatile synthesis of MQW perovskites provides freedom to control the crystallinity and morphology of the emission layer. It is demonstrated that the inclusion of chloride can further improve the crystallization and consequently the optical properties of the Cs-based MQW perovskites, inducing a low turn-on voltage of 2.0 V, a maximum external quantum efficiency of 3.7%, a luminance of ≈440 cd m^{-2} at 4.0 V. These results suggest that the Cs-based MQW LED is among the best performing red perovskite LEDs. Moreover, the LED device demonstrates a record lifetime of over 5 h under a constant current density of 10 mA cm^{-2}. This work suggests that the MQW perovskites is a promising platform for achieving high performance visible-range electroluminescence emission through high-throughput processing methods, which is attractive for low-cost lighting and display applications.

Organometal halide perovskite light-emitting diodes (PeLEDs) have received considerable attention due to their potential for solution-processed, low-cost displays, and lighting sources.[1–4] In order to achieve high efficiency PeLEDs, it is a challenge to fabricate highly emissive thin perovskite layers with uniform film morphology. The efficiency of 3D perovskites based LEDs is mainly limited by the nonradiative loss channels caused by defects or pin-holes in the emission layer.[2] 2D organometal perovskites are natural formed quantum wells with excellent film morphology, but previous study showed that their photoluminescence (PL) efficiency is very low at room temperature due to strong exciton–phonon interaction.[5–7] Recent results showed that the photoluminescence quantum efficiency (PLQE) of the 2D perovskites can be significantly enhanced when multiple quantum well (MQW) structure forms with energy cascade.[8] The high PLQE of the MQW perovskites is due to the fast energy transfer from the large bandgap QWs to small bandgap QWs where efficient radiative decay occurs.[8,9] Consequently, the MQW-based PeLED can have high external quantum efficiency (EQE) up to 11.7% in near-infrared (NIR).[8] An interesting question is whether the MQW LEDs can achieve similar high performance in the visible range.

For visible emission PeLEDs, efficient green emission has been demonstrated by using 3D $CH_3NH_3PbBr_3$ films, while the EQE of red 3D perovskite LEDs is only 0.2%.[1] The low efficiency of the red PeLEDs is mainly due to low PLQEs of the perovskite emission layers caused by the halide phase segregation of the I—Br mixed perovskite films used.[10–12] Alternatively, $CsPbI_3$ perovskite nanocrystals with high PLQE and pure color emission seem to be a good candidate for red light emitters.[13] By using atomic layer deposition (ALD) and cross-linking method, $CsPbI_3$ nanocrystal-based red LEDs showed a 5.7% EQE and a maximum luminance of 206 cd m^{-2}.[14] The study demonstrates the promise of exploiting quantum confinement effects in achieving high performance red PeLEDs, although the device fabrication process still involves steps (e.g., ALD) that are time consuming and difficult to scale up.

In this work, we demonstrate a facile and scalable process to achieve high performance red PeLEDs by introducing inorganic cesium (Cs^+) into MQW perovskites. The MQW structure facilitates the formation of cubic $CsPbI_3$ perovskites at low temperature, and the Cs-based QWs provide pure and stable red electroluminescence (EL). With the MQW perovskites there is no need to use ALD coated passivation layer, and the electron- and hole- transport layers can all be deposited through rapid

S. Zhang, Dr. C. Yi, Dr. N. Wang, Y. Sun, W. Zou, Y. Wei, Y. Cao, Y. Miao, Dr. R. Li, Dr. Y. Yin, Prof. J. Wang, Prof. W. Huang
Key Laboratory of Flexible Electronics (KLOFE) & Institute of Advanced Materials (IAM)
Jiangsu National Synergetic Innovation Center for Advanced Materials (SICAM)
Nanjing Tech University (NanjingTech)
30 South Puzhu Road, Nanjing 211816, China
E-mail: iamjpwang@njtech.edu.cn; wei-huang@njtech.edu.cn

Prof. N. Zhao
Department of Electronic Engineering
The Chinese University of Hong Kong
New Territories, Hong Kong

Prof. W. Huang
Key Laboratory for Organic Electronics and Information Displays & Institute of Advanced Materials (IAM)
Jiangsu National Synergetic Innovation Center for Advanced Materials (SICAM)
Nanjing University of Posts & Telecommunications
9 Wenyuan Road, Nanjing 210023, China

DOI: 10.1002/adma.201606600

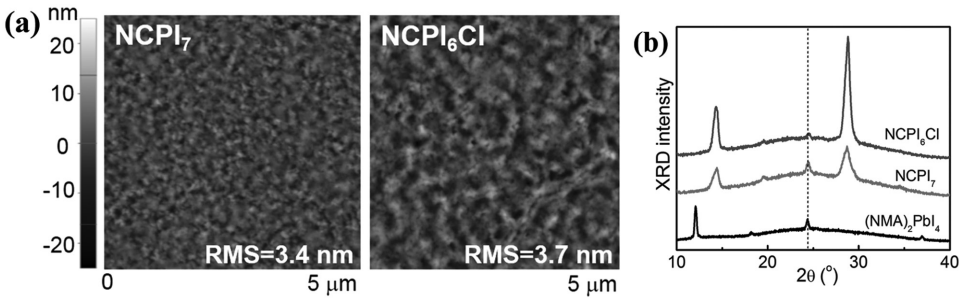

Figure 1. Perovskite MQW films. a) AFM height image of the $NCPI_7$ and $NCPI_6Cl$ MQW films. b) XRD data of the $(NMA)_2PbI_4$, $NCPI_7$, and $NCPI_6Cl$ films.

solution casting processes. Furthermore, the versatile synthesis of MQW perovskites provides freedom to control the crystallinity and morphology of the emission layer. For instance, we demonstrate that the inclusion of chloride can further improve the crystallization and consequently the optical properties of the Cs-based MQW perovskites, inducing a maximum EQE of 3.7%, a luminance of ≈440 cd m^{-2} at a low voltage of 4.0 V, and a record lifetime of over 5 h under a constant current density of 10 mA cm^{-2}.

The red emission MQW perovskite films are prepared similar to our previously reported method.[8] A precursor solution of 1-naphthylmethylamine iodide, cesium iodide (CsI), and PbI_2 with a molar ratio of 2:1:2 dissolved in a mixed solution of *N*,*N*-dimethylformamide (DMF) and dimethyl sulfoxide (volume ratio, 9:1) was used to deposit red emission MQW perovskite films, which are abbreviated as $NCPI_7$ films below. After spin-coating, the film is annealed at 110 °C for ≈ 5 min in a nitrogen glove box. Atomic force microscopy (AFM) measurement shows the $NCPI_7$ film is very uniform, with 3.4 nm root-mean-square roughness (**Figure 1**a).

We first study the structure properties of the $NCPI_7$ film by using X-ray diffraction (XRD) technique (Figure 1b). The $NCPI_7$ film exhibits strong peaks at ≈14.4° and 28.8°, which is in accordance with the typical $CsPbI_3$ perovskite α-phase,[15,16] indicating the formation of large-*n* QWs close to crystalline $CsPbI_3$ in our low-temperature-processed $NCPI_7$ film. We also note a weak XRD peak at 24° with the $NCPI_7$ film, consistent with the existence of the $n = 1$ QW ($(NMA)_2PbI_4$ (also shown in Figure 1b). Therefore, the XRD result suggests that the $NCPI_7$ film is a mixture of $n = 1$ QW with large-*n* QW perovskite domains.

To further reveal the structure of the $NCPI_7$ film, optical characterization is fulfilled. **Figure 2**a shows absorbance and PL spectra of $NCPI_7$ MQW film. The absorption spectrum of the $NCPI_7$ film shows a strong exciton absorption peak at 2.44 eV and shoulders at 2.24 and 1.86 eV, which suggests that the $NCPI_7$ film is a mixture of perovskite QWs with different bandgaps. The different absorption intensities indicate that $(NMA)_2PbI_4$ ($n = 1$ QW) is the majority component of the $NCPI_7$ film, and there are also small fractions of $n = 2$ QW ($(NMA)_2(CsPbI_3)PbI_4$) and larger-*n* QWs in the $NCPI_7$ film.[8] Accordingly, the PL spectrum shows several emission peaks at 2.42, 2.22, and 1.81 eV, which correspond well with the absorption peaks. The strongest absorption peak (2.44 eV) presents very weak PL emission which can only be distinguishable in logarithmic scale. And the dominating PL emission peak (1.81 eV) is from the large-*n* QW, which is slightly blue-shifted to the PL emission peak of 3D $CsPbI_3$ perovskite (≈1.78 eV) (Figure S1, Supporting Information). The absorption and PL results indicate that energy transfer process occurs from large bandgap QWs to small bandgap QWs. PL excitation (PLE) measurements on the $NCPI_7$ film show that different emissions share same excitation peaks at 2.44 and 2.25 eV (Figure 2b), confirming that the process of energy transfer from $n = 1$ and $n = 2$ QWs contributes to the lower energy emissions. Figure 2c shows that the PL at different emission peaks have markedly different lifetimes. The PL lifetime increases as the emission photon energy decreases. The time-resolved PL measurements are consistent with a fast cascade energy transfer from the majority of $n = 1$ QWs to large-*n* QWs which may have much higher PL efficiencies. Figure 2d shows that the $NCPI_7$ film has relatively high PLQEs, ≈15%, even at very low excitation intensities. Those optical characterization results suggest that the $NCPI_7$ films have similar MQW structures as NIR emission $NFPI_7$ MQWs,[8] which can give efficient radiative decay by cascade energy transfer and exciton confinement in the large-*n* QWs. We note that although $CsPbI_3$ cubic perovskite geometry is known to be formed at high temperature (>300 °C),[17] our low temperature processing results suggest that the MQW structure can facilitate the formation of large-*n* QWs close to the $CsPbI_3$.[18] This can be due to entropic stabilization of mixed cations, which has been observed in the mixtures of formamidinium (FA)–methylammonium or FA–Cs cations of perovskite solar cells.[18,19]

The device architecture of red MQW LED based on the $NCPI_7$ film is indium tin oxide/polyethylenimine ethoxylated modified zinc oxide (ZnO, ≈20 nm)/perovskite MQWs (≈60 nm)/poly(9,9-dioctyl-fluorene-*co*-*N*-(4-butylphenyl)diphenylamine) (TFB, ≈60 nm)/molybdenum oxide (MoO_x, ≈7 nm)/gold (Au, ≈60 nm). The energy-level diagram is shown in **Figure 3**a, wherein the energy level values for $NCPI_7$ film were estimated by ultraviolet photoelectron spectroscopy (UPS) (Figure S2, Supporting Information) and optical measurements. The fabrication details can be found in the Experimental Section.

The device EL spectrum, current density–voltage–luminance (*J*–*V*–*L*) and EQE characteristics are also shown in Figure 3. The EL emission peak is at 689 nm (Figure 3b), which is ≈12 nm blue-shifted to the EL emission of 3D $CsPbI_3$ LED (Figure S3, Supporting Information). The LED device exhibits very pure red emission with Commission Internationale de l'Eclairage (CIE) color coordinates of (0.73, 0.27) (Figure 3c), which is almost the

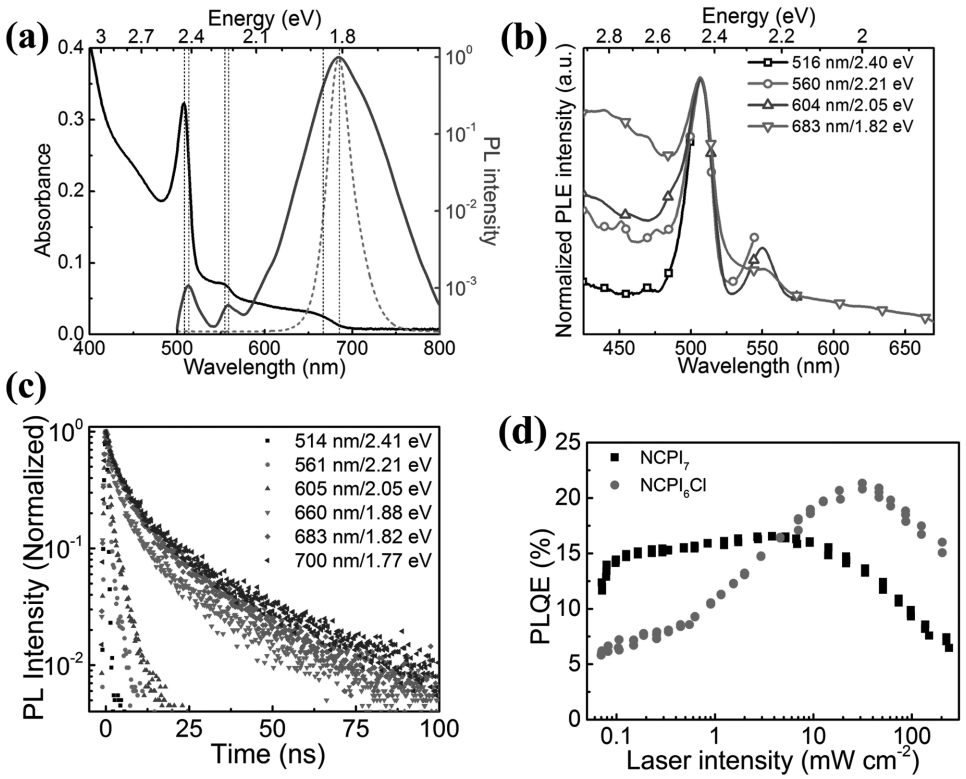

Figure 2. Optical properties of $NCPI_7$ and $NCPI_6Cl$ films. a) Absorption and PL (445 nm excitation) spectra of the $NCPI_7$ MQW film deposited onto quartz substrates. The PL spectrum is normalized in log scale (blue curve) and linear scale (red dashed curve). b) PL excitation spectra of the $NCPI_7$ MQW film at various emission energies. c) Time-resolved PL decay transients of the $NCPI_7$ MQW film at different emission energies. Emission photons with smaller energy show longer PL decay time. d) Excitation-intensity-dependent PLQE of the $NCPI_7$ and $NCPI_6Cl$ MQW film.

right corner of the CIE coordinates. The shapes of EL spectra do not change at different bias voltages (Figure S4, Supporting Information), unlike mixed I—Br 3D perovskite LEDs which show red-shifted EL emission upon device operation.[14] The $NCPI_7$–MQW LED turns on at a voltage of 2.4 V (Figure 3d) and a luminance of 55 cd m^{-2} can be achieved at a voltage of 4 V. The EQE of the LED reaches 2.4% at 3.1 V with a luminance of 15 cd m^{-2} (Figure 3e). The average peak EQE of 43 devices is 1.5% with a relative standard deviation of 21%, showing good reproducibility of the device performance (Figure 3f).

Inclusion of chlorides in perovskite precursors have been shown to enhance the solar cell performance by improving the film optoelectronic properties.[20–22] Here we explore the similar strategy to further improve the performance of our MQW perovskite LEDs. By replacing the CsI with CsCl in the precursor solution, we can obtain MQW films (abbreviated as $NCPI_6Cl$ below) with better optical properties than $NCPI_7$ MQW film. The absorption, PL and PLE spectra of the $NCPI_6Cl$ film exhibit consistent results as $NCPI_7$ film (Figure S5, Supporting Information), suggesting the $NCPI_6Cl$ film consists of similar self-organized MQWs as those in the $NCPI_7$ film.

It has been widely observed that Cl incorporation can improve the crystallinity in 3D perovskites.[23] We find that the similar improvement occurs in the formation of MQW perovskites. X-ray photoelectron spectroscopy (XPS) data show the presence of trace amount of chloride ions in the MQW perovskites (Figure S6, Supporting Information). The Cs atomic ratio in $NCPI_6Cl$ film is 11.1%, while that in $NCPI_7$ film is 7.5%, indicating the incorporation of Cl favors the growth of larger-*n* QWs in the MQW perovskites. This hypothesis is supported by the XRD measurement, where $NCPI_6Cl$ shows much narrower XRD peaks (Figure 1b). The full-width half maximum value of XRD peak at 14.4° of $NCPI_6C1$ and $NCPI_7$ are 0.58° and 0.75°, respectively. The average crystal sizes of $NCPI_6Cl$ and $NCPI_7$ are 15 and 10 nm, respectively, which is also consistent with the AFM measurement (Figure 1a). All these results suggest that the inclusion of chlorides can change the crystal formation kinetics in the Cs-based MQW perovskites.[24] We believe the improvement mechanism of MQW perovskite crystallinity by incorporating chlorine is similar to the case of 3D perovskites,[25–27] i.e., chlorine atoms participate in the formation of an intermediate phase, followed by exchanged by iodine atoms and repelled out of the perovskite network. The existence of the intermediate phase promotes the formation of compact films with relatively large crystalline domains. We note however that in the case of 3D $MAPbI_3$ perovskite, chlorine can easily escape from the perovskite film through sublimation of MACl or volatilization of HCl and MA gas. In the case of the MQW structure, the organic cations are bulky; therefore, the sublimation and volatilization processes are suppressed. This results in a higher content of chlorine residue in the MQW film. It is also worth mentioning that it has been theoretically and experimentally validated that chlorine residue

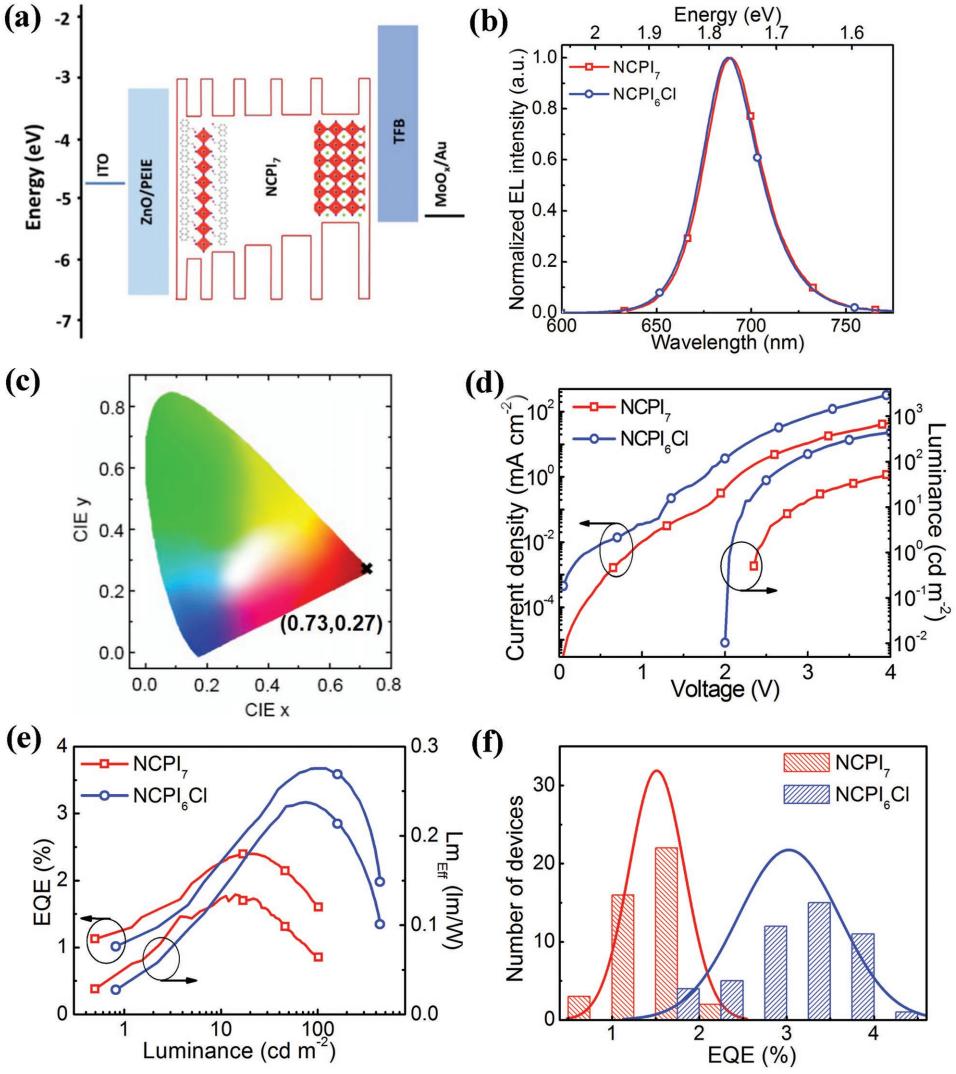

Figure 3. Device characteristics of the $NCPI_7$ and $NCPI_6Cl$ MQW perovskite LEDs. a) Flat-band energy level diagram ($NCPI_7$). The energy level values besides $NCPI_7$ were taken from the literature.[2] b) EL spectra of the $NCPI_7$ and $NCPI_6Cl$ devices. c) Corresponding CIE coordinate of $NCPI_7$ device. d) Dependence of current density and luminance on the driving voltage. e) EQE and luminous efficacy versus luminance. f) Histograms of peak EQEs measured from $NCPI_7$ and $NCPI_6Cl$ devices.

can positively impact the electronic properties of perovskite films by passivating the defects and reduce charge recombination.[28–30] Transient PL measurement shows that the carrier lifetime is increased in $NCPI_6Cl$ (Figure 2; Figure S5, Supporting Information), indicating Cl helps to reduce the defects in the MQW structures.[31] As a result, the maximum PLQEs of $NCPI_6Cl$ film is enhanced, reaching up to ≈20% (Figure 2d).

The EL emission peak of LEDs based on the $NCPI_6Cl$ film is 688 nm (Figure 3b), which is almost same as that of the $NCPI_7$ devices. The champion $NCPI_6Cl$ LED turns on at a low voltage of 2.0 V, which is 0.4 V lower than the $NCPI_7$ device. The lower turn-on voltage can be due to the better charge transport in the $NCPI_6Cl$ film with improved crystallinity. A high luminance of ≈440 cd m^{-2} is achieved at 4.0 V. The EQE reaches to 3.7% at 2.8 V with a luminance of ≈100 cd m^{-2}, which is increased by over 50% compared with the $NCPI_7$ devices. The EQE enhancement of the $NCPI_6Cl$ device is consistent with the improved PLQE of the $NCPI_6Cl$ film (Figure 2d). The EQE histogram for 48 devices shows an average peak EQE of 3.0% with a relative standard deviation of 19%. Moreover, the peak luminous efficacy of $NCPI_6Cl$ LED is 0.24 lm W^{-1} at a brightness of ≈75 cd m^{-2}. These results suggest that our Cs-based MQW LED is among the best performing red perovskite LEDs (Table S1, Supporting Information). We note that the $NCPI_6Cl$ MQW LEDs have excellent operation stability. The EQE of $NCPI_6Cl$ devices dropped to half of the initial value after ≈5 h under a constant driving current density of 10 mA cm^{-2} (**Figure 4**a). The lifetime is doubled compared to previous reported NIR emission MQW perovskite LEDs under the same driving condition,[8] and is a new record for PeLEDs. The shape of the EL spectra remains unchanged upon long-term bias (Figure 4b). We believe that the improved device reliability can be attributed to the intrinsic stability of Cs-based perovskite films.[15,18]

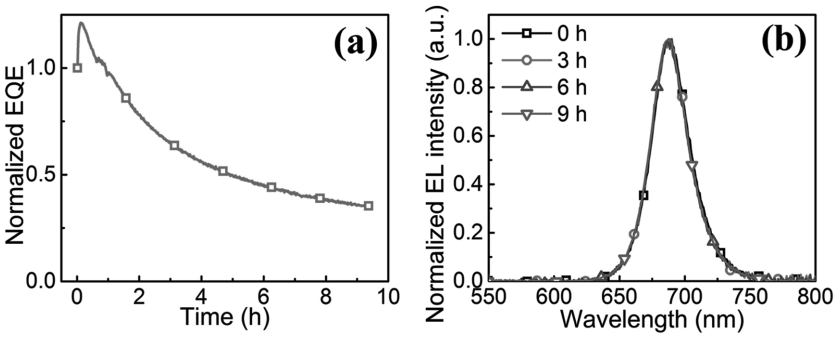

Figure 4. Stability measurements on $NCPI_6Cl$ MQW perovskite LEDs. a) Normalized EQE for an $NCPI_6Cl$ EL device tested at a constant current density of 10 mA cm^{-2}. b) EL spectra of the $NCPI_6Cl$ device upon long-term bias.

We show that by using cesium-based self-organized perovskite MQWs, efficient and high-brightness red LEDs with good stability can be achieved. The inclusion of chloride can promote the formation of perovskite MQWs with high crystallization and further improved optical properties. Our results demonstrate that the MQW perovskites is a promising platform that allows achieving high performance visible-range EL emissions through high-throughput manufacturing processes, which is attractive for low-cost lighting and display applications.

Experimental Section

Synthesis and Materials Preparation: Colloidal ZnO nanocrystals were synthesized by a solution-precipitation process[32] with some modifications. $NCPI_7$ and $NCPI_6Cl$ precursor solutions were prepared similar to the previously reported method.[8] $CsPbI_3$ precursor solutions were prepared by dissolving CsI and PbI_2 with molar ratio of 1:1 in DMF (10 wt%).

Device Fabrication: A detailed description of device fabrication can be found elsewhere.[8] Here, the TFB layers were deposited from an *m*-xylene solution (13 mg mL^{-1}) at 2000 rpm.

Device Characterization: A detailed description of all perovskite LED device characterizations can be found elsewhere.[8] The devices were swept from zero bias to forward bias at 0.05 V s^{-1}. The time evolution of EQEs was measured using the same testing system at room temperature in a nitrogen-filled glove box.

Film Characterization: AFM images were taken using a Park XE7 atomic force microscope in noncontact mode. UV–vis absorbance and PL spectra of the perovskite films were measured using an Agilent Cary 5000 UV–vis spectrophotometer with an integrating sphere and a HITACHI F-4600 fluorescent spectrophotometer, respectively. The excitation spectra and time resolved fluorescence spectra of the perovskite films were obtained by using an Edinburgh Instruments (FLS920) spectrometer. Here, the time-resolved PL excitation fluence is ≈4 nJ cm^{-2} from an EPL-405 pulsed diode laser. A three-step technique combining laser, optical fiber, spectrometer, and integrating sphere was used to obtain PLQE of perovskite films.[33] UPS and XPS spectra were collected on a Thermo ESCALAB-250Xi spectrometer (He I UV radiation source, 21.2 eV) and a Thermo ESCALAB 250 equipment, respectively.

Supporting Information

Supporting Information is available from the Wiley Online Library or from the author.

Acknowledgements

S.Z. and C.Y. contributed equally to this work. This work was financially supported by the National Basic Research Program of China-Fundamental Studies of Perovskite Solar Cells (2015CB932200), the Natural Science Foundation of Jiangsu Province, China (BK20131413, BK20140952, BK20150043, and BK20161008), the National Natural Science Foundation of China (11474164 and 61405091), the Joint Research Program between China and European Union (2016YFE0112000), the Jiangsu Specially-Appointed Professor program, the Synergetic Innovation Center for Organic Electronics and Information Displays. The authors thank H. He and J. Zhang for the assistance of the PLE and TCSPC measurements, and Y. Liu for the UPS and XPS measurements.

Keywords

cesium, light-emitting diodes, multiple quantum wells, perovskites

Received: December 6, 2016
Revised: January 11, 2017
Published online:

[1] Z.-K. Tan, R. S. Moghaddam, M. L. Lai, P. Docampo, R. Higler, F. Deschler, M. Price, A. Sadhanala, L. M. Pazos, D. Credgington, F. Hanusch, T. Bein, H. J. Snaith, R. H. Friend, *Nat. Nanotechnol.* **2014**, *9*, 687.
[2] J. Wang, N. Wang, Y. Jin, J. Si, Z.-K. Tan, H. Du, L. Cheng, X. Dai, S. Bai, H. He, Z. Ye, M. L. Lai, R. H. Friend, W. Huang, *Adv. Mater.* **2015**, *27*, 2311.
[3] L. Cheng, Y. Cao, R. Ge, Y.-Q. Wei, N.-N. Wang, J.-P. Wang, W. Huang, *Chin. Chem. Lett.* **2017**, *28*, 29.
[4] N. Wang, J. Si, Y. Jin, J. Wang, W. Huang, *Acta Chim. Sinica* **2014**, *73*, 171.
[5] X. Hong, T. Ishihara, A. V. Nurmikko, *Phys. Rev. B* **1992**, *45*, 6961.
[6] K. Gauthron, J. S. Lauret, L. Doyennette, G. Lanty, A. Al Choueiry, S. J. Zhang, A. Brehier, L. Largeau, O. Mauguin, J. Bloch, E. Deleporte, *Opt. Express* **2010**, *18*, 5912.
[7] R. Li, C. Yi, R. Ge, W. Zou, L. Cheng, N. Wang, J. Wang, W. Huang, *Appl. Phys. Lett.* **2016**, *109*, 151101.
[8] N. Wang, L. Cheng, R. Ge, S. Zhang, Y. Miao, W. Zou, C. Yi, Y. Sun, Y. Cao, R. Yang, Y. Wei, Q. Guo, Y. Ke, M. Yu, Y. Jin, Y. Liu, Q. Ding, D. Di, L. Yang, G. Xing, H. Tian, C. Jin, F. Gao, R. H. Friend, J. Wang, W. Huang, *Nat. Photonics* **2016**, *10*, 699.
[9] M. Yuan, L. N. Quan, R. Comin, G. Walters, R. Sabatini, O. Voznyy, S. Hoogland, Y. Zhao, E. M. Beauregard, P. Kanjanaboos, Z. Lu, D. H. Kim, E. H. Sargent, *Nat. Nanotechnol.* **2016**, *11*, 872.
[10] E. T. Hoke, D. J. Slotcavage, E. R. Dohner, A. R. Bowring, H. I. Karunadasa, M. D. McGehee, *Chem. Sci.* **2014**, *6*, 613.
[11] Y.-H. Kim, H. Cho, J. H. Heo, T.-S. Kim, N. Myoung, C.-L. Lee, S. H. Im, T.-W. Lee, *Adv. Mater.* **2015**, *27*, 1248.
[12] J. H. Noh, S. H. Im, J. H. Heo, T. N. Mandal, S. I. Seok, *Nano Lett.* **2013**, *13*, 1764.
[13] S. Yakunin, L. Protesescu, F. Krieg, M. I. Bodnarchuk, G. Nedelcu, M. Humer, G. De Luca, M. Fiebig, W. Heiss, M. V. Kovalenko, *Nat. Commun.* **2015**, *6*, 8056.
[14] G. Li, F. W. R. Rivarola, N. J. L. K. Davis, S. Bai, T. C. Jellicoe, F. de la Peña, S. Hou, C. Ducati, F. Gao, R. H. Friend, N. C. Greenham, Z.-K. Tan, *Adv. Mater.* **2016**, *28*, 3528.

[15] G. E. Eperon, G. M. Paternò, R. J. Sutton, A. Zampetti, A. A. Haghighirad, F. Cacialli, H. J. Snaith, *J. Mater. Chem. A* **2015**, *3*, 19688.
[16] Z. Li, M. Yang, J.-S. Park, S.-H. Wei, J. J. Berry, K. Zhu, *Chem. Mater.* **2016**, *28*, 284.
[17] C. K. Møller, *Nature* **1958**, *182*, 1436.
[18] C. Yi, J. Luo, S. Meloni, A. Boziki, N. Ashari-Astani, C. Grätzel, S. M. Zakeeruddin, U. Röthlisberger, M. Grätzel, *Energy Environ. Sci.* **2016**, *9*, 656.
[19] N. Pellet, P. Gao, G. Gregori, T.-Y. Yang, M. K. Nazeeruddin, J. Maier, M. Grätzel, *Angew. Chem., Int. Ed.* **2014**, *53*, 3151.
[20] M. M. Lee, J. Teuscher, T. Miyasaka, T. N. Murakami, H. J. Snaith, *Science* **2012**, *338*, 643.
[21] S. D. Stranks, G. E. Eperon, G. Grancini, C. Menelaou, M. J. P. Alcocer, T. Leijtens, L. M. Herz, A. Petrozza, H. J. Snaith, *Science* **2013**, *342*, 341.
[22] H. Zhou, Q. Chen, G. Li, S. Luo, T. Song, H.-S. Duan, Z. Hong, J. You, Y. Liu, Y. Yang, *Science* **2014**, *345*, 542.
[23] Y. Zhou, O. S. Game, S. Pang, N. P. Padture, *J. Phys. Chem. Lett.* **2015**, *6*, 4827.
[24] Q. Chen, H. Zhou, Y. Fang, A. Z. Stieg, T.-B. Song, H.-H. Wang, X. Xu, Y. Liu, S. Lu, J. You, P. Sun, J. McKay, M. S. Goorsky, Y. Yang, *Nat. Commun.* **2015**, *6*, 7269.
[25] S. T. Williams, F. Zuo, C.-C. Chueh, C.-Y. Liao, P.-W. Liang, A. K.-Y. Jen, *ACS Nano* **2014**, *8*, 10640.
[26] G. Li, T. Zhang, N. Guo, F. Xu, X. Qian, Y. Zhao, *Angew. Chem., Int. Ed.* **2016**, *55*, 13460.
[27] H. Yu, F. Wang, F. Xie, W. Li, J. Chen, N. Zhao, *Adv. Funct. Mater.* **2014**, *24*, 7102.
[28] C. Quarti, E. Mosconi, P. Umari, F. De Angelis, *Inorg. Chem.* **2017**, *56*, 74.
[29] P. Delugas, A. Filippetti, A. Mattoni, *Phys. Rev. B* **2015**, *92*, 45301.
[30] D. E. Starr, G. Sadoughi, E. Handick, R. G. Wilks, J. H. Alsmeier, L. Köhler, M. Gorgoi, H. J. Snaith, M. Bär, *Energy Environ. Sci.* **2015**, *8*, 1609.
[31] W.-J. Yin, H. Chen, T. Shi, S.-H. Wei, Y. Yan, *Adv. Electron. Mater.* **2015**, *1*, 1500044.
[32] L. Qian, Y. Zheng, K. R. Choudhury, D. Bera, F. So, J. Xue, P. H. Holloway, *Nano Today* **2010**, *5*, 384.
[33] J. C. de Mello, H. F. Wittmann, R. H. Friend, *Adv. Mater.* **1997**, *9*, 230.